# Self-affine scaling from non-integer phase-space partition in $\pi^+$p and K$^+$p Collisions at 250 GeV/$c$

## EHS/NA22 Collaboration

N.M. Agababyan[8], M.R. Atayan[8,a], Chen Gang[7,b], E.A. De Wolf[1,c], K. Dziunikowska[2,d],
A.M.F. Endler[5], Gao Yanmin[7], Z.Sh. Garutchava[6], H.R. Gulkanyan[8,a], R.Sh. Hakobyan[8,a],
D. Kisielewska[2,d], W. Kittel[4], Liu Lianshou[7], S.S. Mehrabyan[8,a], Z.V. Metreveli[6], K. Olkiewicz[2,d],
F.K. Rizatdinova[3], E.K. Shabalina[3], L.N. Smirnova[3], M.D. Tabidze[6], L.A. Tikhonova[3],
A.V. Tkabladze[6], A.G. Tomaradze[6], F. Verbeure[1], Wu Yuanfang[7], S.A. Zotkin[3]

[1] Department of Physics, Universitaire Instelling Antwerpen, B-2610 Wilrijk, Belgium
[2] Institute of Physics and Nuclear Techniques of Academy of Mining and Metallurgy and Institute of Nuclear Physics, PL-30055 Krakow, Poland
[3] Nuclear Physics Institute, Moscow State University, RU-119899 Moscow, Russia
[4] High Energy Physics Institute Nijmegen (HEFIN), University of Nijmegen/NIKHEF, NL-6525 ED Nijmegen, The Netherlands
[5] Centro Brasileiro de Pesquisas Fisicas, BR-22290 Rio de Janeiro, Brazil
[6] Institute for High Energy Physics of Tbilisi State University, GE-380086 Tbilisi, Georgia
[7] Institute of Particle Physics, Hua-Zhong Normal University, Wuhan 430070, China
[8] Institute of Physics, AM-375036 Yerevan, Armenia

## Abstract

A factorial-moment analysis with real (integer and non-integer) phase space partition is applied to $\pi^+$p and K$^+$p collisions at 250 GeV/$c$. Clear evidence is shown for self-affine rather than self-similar power-law scaling in multiparticle production. The three-dimensional self-affine second-order scaling exponent is determined to be 0.061±0.010.

[a] Supported by the Government of the Republic of Armenia, contractnumber 94-496

[b] Permanent address: Department of Physics, Jingzhou Teacher's College, Hubei 434100, China

[c] Onderzoeksdirecteur NFWO, Belgium

[d] Supported by the Polish State Committee for Scientific Research

# 1   Introduction

Classical non-Abelian theories show non-linear behavior [1] and the non-linear development of a classical non-Abelian system can be determined numerically [2]. Although extension to a quantum theory as QCD is far from trivial, non-linearity is inherent also to QCD shower development.[3]

The first experimental evidence for non-linear behavior in high-energy multiparticle production came from multiplicity fluctuations in a JACEE event recorded in 1983 [4,5]. In this event, the total multiplicity is about one thousand and the fluctuations in small rapidity bins are 2 times average. In 1987, NA22 [6] found an event in which the fluctuation in a small rapidity bin is as high as 60 times average.

To be able to decide whether these fluctuations are dynamical, i.e. larger than expected from Poisson noise, Białas and Peschanski [6] suggested to use factorial moments (FM), defined as

$$F_q(\delta) = \frac{1}{M} \sum_{m=1}^{M} \frac{\langle n_m(n_m - 1) \cdots (n_m - q + 1)\rangle}{\langle n_m \rangle^q}. \tag{1}$$

In the above equation, $M$ is the partition number of a fixed phase space region $\Delta$ under consideration, $\delta = \Delta/M$ is the size of a sub-cell, $n_m$ is the number of (charged) particles falling into the $m$th sub-cell. The authors show, if the power-law scaling

$$F_q(\delta) \propto \delta^{-\phi_q} \tag{2}$$

holds when $\delta \to 0$, then dynamic self-similar fluctuations are present in multiparticle production.

In the following, the behavior of $F_q$ in ever smaller phase-space cells $\delta$ was studied in almost all high-energy experiments on lepton-lepton, lepton-nucleon, hadron-hadron and nucleus-nucleus collisions and approximate scaling was established (for recent reviews see [7]). It has been pointed out [8], however, that the anisotropy of phase space [9] has to be taken into account and that the multiparticle final state in a high energy hadron-hadron collision may be 'self-affine' [10] rather than self-similar.

In this note we apply a self-affine analysis to the NA22 data on $\pi^+$p and K$^+$p collisions at 250 GeV/$c$, where, in addition, the phase-space partition $M$ of (1) is generalized to real (i.e. also non-integer) values. This method reduces the $\chi^2$/NDF values by a factor of 2 with respect to the limitation to integer values and grants clear evidence for the presence of dynamical self-affine fluctuations in these collisions. The three-dimensional self-affine scaling exponent is determined to be $\phi_2^{3D} = 0.061 \pm 0.010$.

# 2   The method

A self-affine transformation in the three phase-space variables denoted $p_a, p_b, p_c$ is defined as $\delta p_a \to \delta p_a/\lambda_a$, $\delta p_b \to \delta p_a/\lambda_b$, $\delta p_c \to \delta p_c/\lambda_c$, with shrinking ratios $\lambda_a$, $\lambda_b$ and $\lambda_c$, respectively. The anisotropy (self-affinity) of a dynamical fluctuation can then be characterized by the so-called roughness or Hurst exponents [10]

$$H_{ij} = \frac{\ln \lambda_i}{\ln \lambda_j}, \qquad (i, j = a, b \quad \text{or} \quad a, c \quad \text{or} \quad b, c), \tag{3}$$

with

$$\lambda_i \leq \lambda_j, \qquad 0 \leq H_{ij} \leq 1. \tag{4}$$

These exponents can be obtained [11] from the experimental $\delta$ dependence observed in the second-order factorial moments in the three corresponding variables. If self-affine fluctuations of multiplicity exist in multiparticle production, exact scaling, i.e. a straight line in $\ln F_q$ versus $\ln M$, should be observed if and only if the $\lambda_i$ are allowed to differ from one another.

The above prediction was checked on our data [12] and on 400 GeV/$c$ pp data.[13] The Hurst exponents for longitudinal-transverse directions were determined to be 0.474±0.056 in the $(y, \varphi)$ plane and 0.477±0.057 in the $(y, p_T)$ plane for 250 GeV/$c$ $\pi^+$p and K$^+$p collisions and 0.74±0.07 in the $(\eta, \varphi)$ plane for 400 GeV/$c$ pp collision. A self-affine higher-dimensional analysis[1] was performed in both cases and the results are confirmative.

However, the original analysis was limited by the small number of combinations of (integer) partitions $M_i$ allowed by condition (3). Therefore, the method (and necessary correction procedure) has recently been generalized to non-integer partitions $M$.[14] In this letter the new method and correction procedure are applied to obtain a precise answer on the question of self-affinity in our data.

## 2.1 Non-integer FM analysis[14]

To be definite, let us consider a one-dimensional analysis in rapidity $y$. In the ideal case, the factorial moments $F_q(\delta y)$ depend on the bin width $\delta y = \Delta y/M$, but not on the position of the bin on the rapidity axis. If that is the case, the result of averaging over all $M$ bins as in (1) is equal to that of averaging over $N$ bins with $N \leq M$. This means that ideally one has $F_2(M) = F_2(N, M)$, where

$$F_2(N, M) = \frac{1}{N} \sum_{m=1}^{N} \frac{\langle n_m(n_m - 1)\rangle}{\langle n_m\rangle^2}, \qquad (N \leq M, \delta y = \Delta y/M) . \tag{5}$$

This equation can be used as the definition of FM for any real (integer or non-integer) value of $M$ [15], provided that the number $N$ of bins used for averaging is taken to be

$$N = M - a, \qquad (0 \leq a < 1). \tag{6}$$

However, even in the central region the rapidity distribution is not flat. The shape of this distribution influences the scaling behavior of the FM. Therefore, the cumulant variable

$$x(y) = \frac{\int_{y_a}^{y} \rho(y')dy'}{\int_{y_a}^{y_b} \rho(y')dy'} \tag{7}$$

was introduced,[16] which has a flat distribution by definition. An additional correction factor has to be introduced again for the FM analysis with non-integer partition.

To see this, let $\Delta$ denote the phase-space region in consideration, $\delta_m$ the $m$th bin, $\rho_1(y_1)$ and $\rho_2(y_1, y_2)$ the one- and two-particle distribution functions, respectively. Then we have

$$\langle n_m\rangle = \int_{\delta_m} \rho_1(y)dy = \frac{\langle n\rangle}{\langle n(n-1)\rangle} \int_\Delta dy_2 \int_{\delta_m} dy_1 \rho_2(y_1, y_2); \tag{8a}$$

$$\langle n_m(n_m - 1)\rangle = \int_{\delta_m} dy_2 \int_{\delta_m} dy_1 \rho_2(y_1, y_2). \tag{8b}$$

---

[1]In the case of NA27, due to lack of momentum measurement, the self-affine analysis was 2D instead of 3D.

After transforming to the cumulant variable, $\langle n_m \rangle$ becomes a constant, independent of $m$. However, comparing the two above equations, it can be seen that due to the difference in the integration region over $y_2$, $\langle n_m(n_m - 1) \rangle$ is in general not constant even though $\langle n_m \rangle$ is. This was experimentally verified on our data.

Note that in the definition of $F_q$ in (1) a horizontal average is taken. When the partition number $M$ is an integer, the horizontal average is over the full region $\Delta$. The variation of $\langle n_m(n_m-1) \rangle / \langle n_m \rangle^2$ is thus smeared out, and no correction is needed. On the contrary, when $M$ is non-integer, the horizontal average is performed over only part of the region and the influence of the variation of $\langle n_m(n_m - 1) \rangle / \langle n_m \rangle^2$ becomes essential.

## 2.2 Correction factor for the $\langle n_m(n_m - 1) \rangle / \langle n_m \rangle^2$ distribution

From the definition of $F_2(N, M)$ in (5) it can be seen that only $N$ bins are included in the horizontal average when $M$ is non-integer ($M = N + a$, $0 < a < 1$). Consequently, only a fraction $r = N/M$ of the full region $\Delta$ is taken into account. We minimize the influence of this by introducing a correction factor $R(r)$ and define [14]

$$F_2(M) = \frac{1}{R(r)} \left( \frac{1}{N} \sum_{m=1}^{N} \frac{\langle n_m(n_m - 1) \rangle}{\langle n_m \rangle^2} \right).$$ (9)

In order to extract $R(r) = R(N/M)$ from the experimental data, let us go back to integer $M$ and calculate $F_2$ averaging only over $N$ of the $M$ bins ($N \leq M$). The result is, in general, a function of both $N$ and $M$. The correction matrix

$$C(N, M) = \frac{\frac{1}{N} \sum\limits_{m=1}^{N} \langle n_m(n_m - 1) \rangle / \langle n_m \rangle^2}{\frac{1}{M} \sum\limits_{m=1}^{M} \langle n_m(n_m - 1) \rangle / \langle n_m \rangle^2} \,, \qquad N = 1, 2, \ldots, M.$$ (10)

is shown in Fig. 1. as a function of $N/M$ for $M = 3, 4, \ldots, 40$. Points for different $M$ lie in a narrow band (mind the scale), so that the correction factors $R_y(r)$, $R_{p_T}(r)$ and $R_\varphi(r)$ can be obtained from an interpolation of $C(N, M)$.

It turns out, however, that the result is very sensitive to the interpolation function. An inappropriate choice of the interpolation function, even inside the narrow $C(N, M)$ band, will be either insufficient in eliminating the "sawteeth" observed in the uncorrected $\ln F_2$ versus $\ln M$ plot or it will over-correct. It is found [14] that when the "sawteeth" lie above the smooth curve of integer $M$, as in the case of $y$ and $p_T$, the upper boundary of the $C(N, M)$ band has to be used for the interpolation. When the "sawteeth" reach from above the smooth curve of integer $M$ to below, as in the case of $\varphi$, the middle of the $C(N, M)$ band has to be used. The interpolation functions used for the three cases are shown as dotted lines in Fig. 1.

Having obtained the correction factor for one-dimensional FM's with non-integer $M$, the correction of higher-dimensional FM's can be obtained from a straight-forward generalisation [14] paying special attention to the overlap regions $(M_1 - N_1)(M_2 - N_2)$ and $(M_1 - N_1)(M_2 - N_2)(M_3 - N_3)$ in the two- and three-dimensional analysis, respectively.

## 3 Results

The details of the EHS spectrometer can be found in [17], those of the trigger and data analysis in [18]. The acceptance criteria and data samples are those already used in [12].

## 3.1 One-dimensional analysis and Hurst parameters

In Fig. 2 are shown the results of a one-dimensional analysis of $\ln F_2$ versus $\ln M$. The first column reproduces the results obtained earlier for integer $M$ [12]. The second column gives the results for real $M$ as defined in (5). It can be seen that the points for non-integer $M$ depart in a "sawtooth pattern" from the curve determined by the points with integer $M$, especially in the cases of $y$ and $p_T$. After correction by $R_y$, $R_{p_T}$ and $R_\varphi$ obtained from the interpolation of the correction matrix $C(N, M)$ above, the results (shown in the third column of Fig. 2) become smooth.

## 3.2 Two-dimensional analysis

The plots for 2-dimensional self-affine FM's are presented in Fig. 3 for $H_{p_T\varphi} = 1$ and $H_{yp_T} = H_{y\varphi} = 0.475$. The same 1-dimensional correction factors $R_y$, $R_{p_T}$ and $R_\varphi$ are used together with the geometrical factors taking care of the overlap regions [14]. The corrected results for $(y, p_T)$ and $(y, \varphi)$ are satisfactory. For $(p_T, \varphi)$ $F_2$ is improved considerably with respect to the original real (integer and non-integer) $M_y$ plot shown in the middle column of Fig. 2.

## 3.3 Three-dimensional analysis

The final 3-D results are presented in Fig. 4. The left figure is the one with integer $M$ obtained before [13]. The right figure is the corrected result of the self-affine analysis with real $M$ together with a linear fit

$$\ln F_2 = A + B \ln M_y . \tag{11}$$

In order to minimize the influence of momentum conservation [19], the fit starts from $M_y = 2$. For the same reason, the non-integer $M$ points are given for $M_y > 2$, only.

It has to be noted that integer M values could be used in our previous analysis only because the Hurst exponents had values close to 0.5 and 1.0, respectively. This was rather accidental, however, and a generalization to real (integer and non-interger) partition [15] is necessary to be able to evaluate other experiments (e.g.[13]). A comparison of integer-M and real-M results in table 1 shows that the slope $B$ itself is unchanged but the error tends to decrease. Furthermore, it can be seen from table 1 that the ratios $\chi^2$/NDF are decreased as compared to those obtained from integer $M$ and at the same time the number of degrees of freedom (NDF) increases largely.

Note that the slope $B$ of (11) is related to $\phi_2$ of (2) via

$$M_{3D} = M_y M_{p_T} M_\varphi = M_y^{1 + \frac{1}{H_{yp_T}} + \frac{1}{H_{y\varphi}}}$$

as

$$\phi_2 = B \left/ \left( 1 + \frac{1}{H_{yp_T}} + \frac{1}{H_{y\varphi}} \right) \right. . \tag{12}$$

From the $B$ value for weighted real $M$ in table 1, we get as the final result for the scaling exponent

$$\phi_2^{3D} = 0.061 \pm 0.010 . \tag{13}$$

# 4    Conclusions

In this paper we presented the results of a self-affine analysis of experimental data on factorial moments generalized to real (integer and non-integer) partition $M$. Correction factors were introduced to minimize the influence of the variation of $\langle n_m(n_m - 1)\rangle$. The corrected results for non-integer $M$ lie on smooth lines interpolating between the integer-$M$ points obtained before.

The results of a three-dimensional self-affine analysis are well fitted by a power law, giving a more general and more precise check of the self-affine power-law scaling of the data than the previous analysis based on integer partition only. The observed behavior is consistent with the fact that the longitudinal direction is privileged over the transverse directions in hadron-hadron collisions. It would be important to use this analysis in the study of QCD parton-shower development in $e^+e^-$ collisions.

# Acknowledgements

# References

[1] S. G. Matinyan, Sov. J. Part. Nucl. **16** (1985) 226.

[2] B. Müller and A. Trayanov, Phys. Rev. Lett. **68** (1992) 3387; C. Gong, Phys. Lett. **B298** (1993) 257; Phys. Rev. **D49** (1994) 2642.

[3] G. Veneziano, Proc. 3rd Workshop on Current Problems in High Energy Particle Theory, Florence 1979, eds. R. Casalbuoni et al. (Johns Hopkins Univ. Press, Baltimore, 1979) p.45.

[4] T. H. Burnett et al. (JACEE), Phys. Rev. Lett. **50** (1983) 2062.

[5] A. Białas and R. Peschanski, Nucl. Phys. **B273** (1986) 703, **B308** (1988) 857.

[6] M. Adamus et al. (NA22), Phys. Lett. **B185** (1987) 200.

[7] P. Bożek, M. Płoszajczak and R. Botet, Phys. Rep. **252** (1995) 101;
E.A. De Wolf, I.M. Dremin and W. Kittel, Phys. Rep. **270** (1996) 1.

[8] Wu Yuanfang and Liu Lianshou, Phys. Rev. Lett **70** (1993) 3197.

[9] L. Van Hove, Phys. Lett. **28B** (1969) 429.

[10] B. Mandelbrot, The Fractal Geometry of Nature, Freeman, NY, 1982; T. Vicsek, Fractal Growth Phenomena, World Scientific, Singapore, 1989.

[11] Wu Yuanfang and Liu Lianshou, Science in China **A38** (1995) 435.

[12] N.M. Agababyan et al. (NA22), Phys. Lett. **B382** (1996) 305.

[13] Wang Shaoshun, Wang Zhaomin and Wu Chong, Phys. Lett. B410 (1997) 323.

[14] Liu Lianshou, Chen Gang and Gao Yanmin, On the factorial moment analysis of high energy experimental data with non-integer partition number, to be published.

[15] Liu Lianshou, Zhang Yang and Wu Yuanfang, Z. Phys. **C69** (1996) 323,

[16] W. Ochs, Z. Phys. **C50** (1991) 339; A. Białas and M. Gazdzichi, Phys.Lett. **B252** (1990) 483.

[17] M. Aguilar-Benitez et al., Nucl. Instrum. Methods **205** (1983) 79.

[18] M. Adamus et al. (NA22), Z. Phys. **C32** (1986) 475.

[19] Liu Lianshou, Zhang Yang and Deng Yue, Z. Phys. **C73** (1997) 535.

Table 1.   The parameter values obtained from a fit of the 3D-data by (11)

| Method | $A$ | $B$ | $\chi^2$/NDF |
|---|---|---|---|
| Without bin-size correlation | | | |
| weighted integer-M | -0.04±0.03 | 0.32±0.03 | 7/4 |
| weighted real-M | -0.01±0.02 | 0.32±0.02 | 19/20 |
| Without bin-size correlation | | | |
| unweighted integer-M | -0.08±0.02 | 0.33±0.03 | 12/4 |
| unweighted real-M | -0.05±0.02 | 0.33±0.02 | 30/20 |
| With bin-size correlation | | | |
| unweighted integer-M | -0.08±0.02 | 0.34±0.02 | 14/4 |
| unweighted real-M | -0.05±0.02 | 0.34±0.02 | 51/20 |

**Figure captions**

Fig. 1  The correction matrix $C(N, M)$ as function of $N/M$ for $M = 3 - 40$ (for the curves see text).

Fig. 2  The one-dimensional plots of $\ln F_2$ versus $\ln M$. The first column are the previous results for integer $M$. The second column are the results of real $M$ as defined in (5). The third column are the results after correction. For easier comparison, the first six integer-M points are indicated as full circles in columns two and three.

Fig. 3  The same as Fig.2 for two-dimensional self-affine FM as a function of $\ln M_y$.

Fig. 4  The three-dimensional plots of $\ln F_2$ versus $\ln M$. The left figure gives the previous results for integer $M$. The right figure gives the corrected results of the self-affine analysis with real $M$ together with a linear fit.
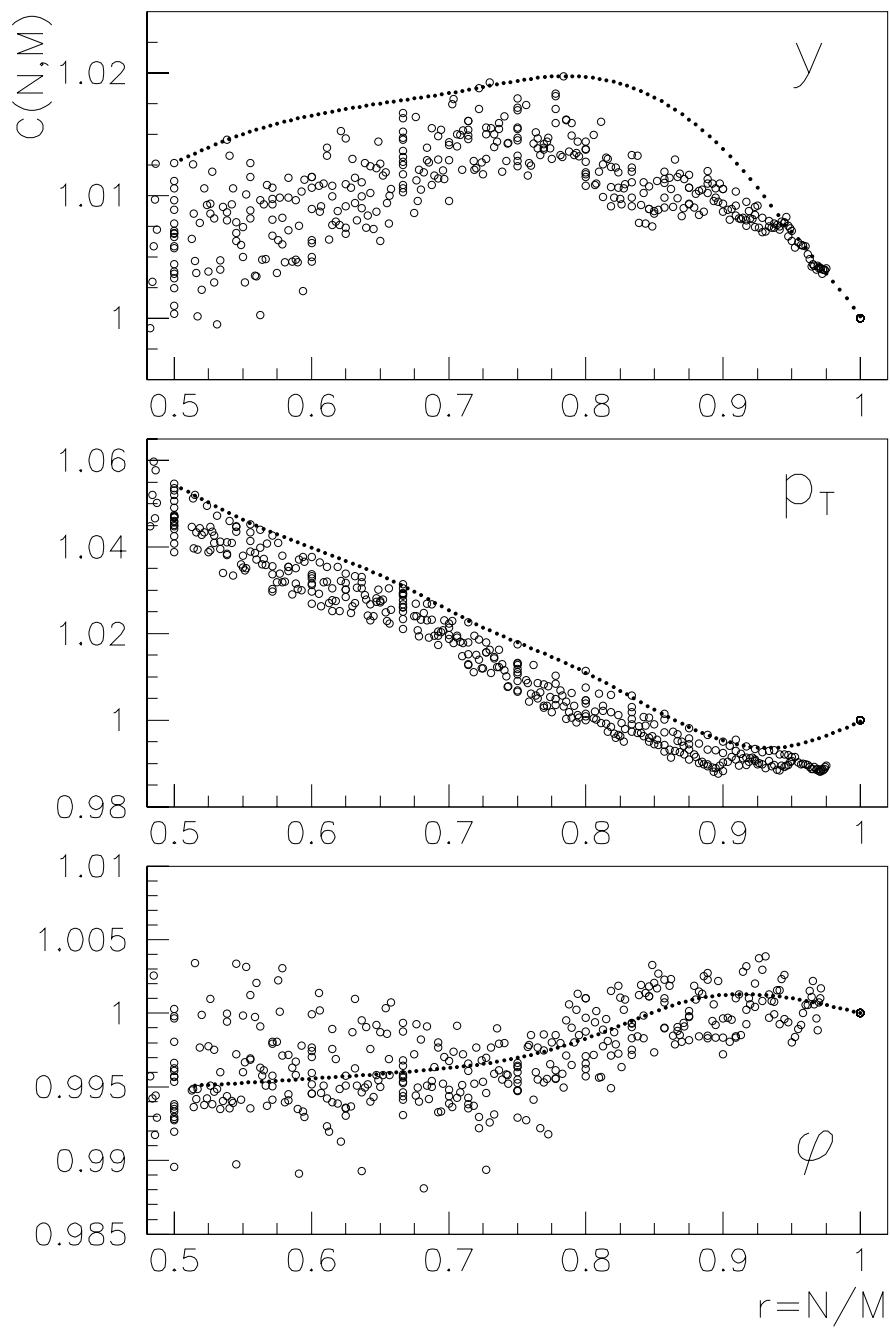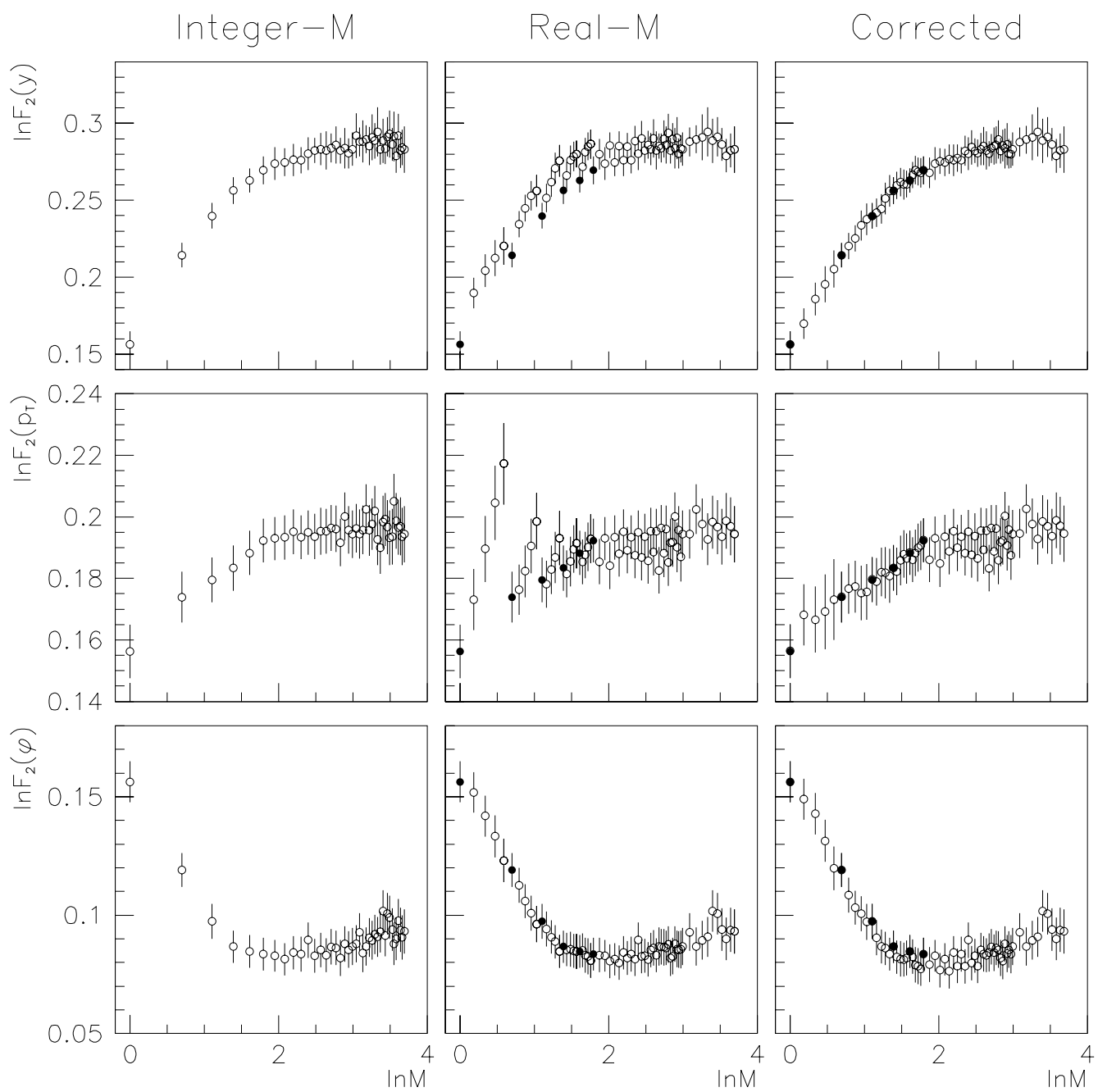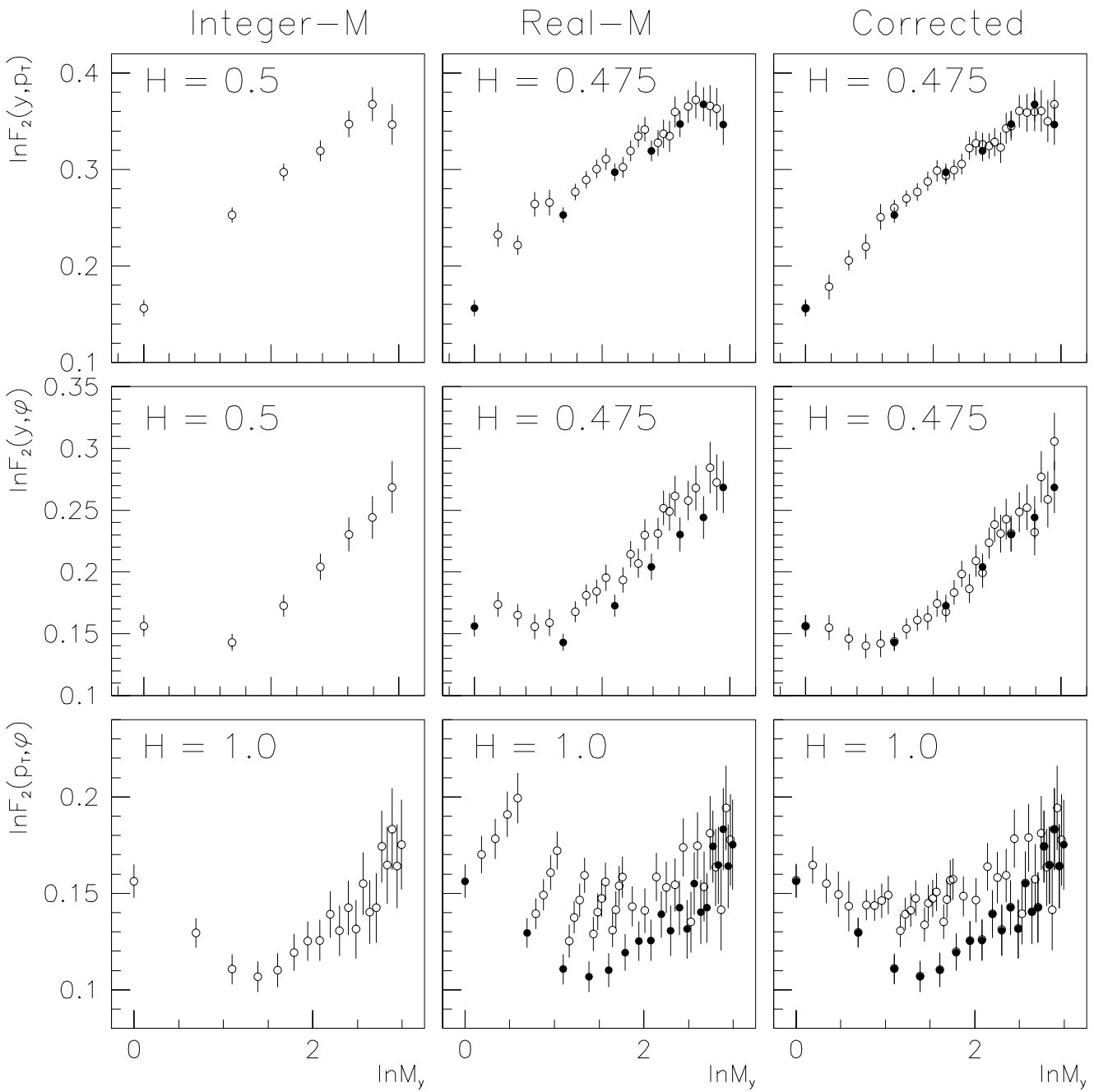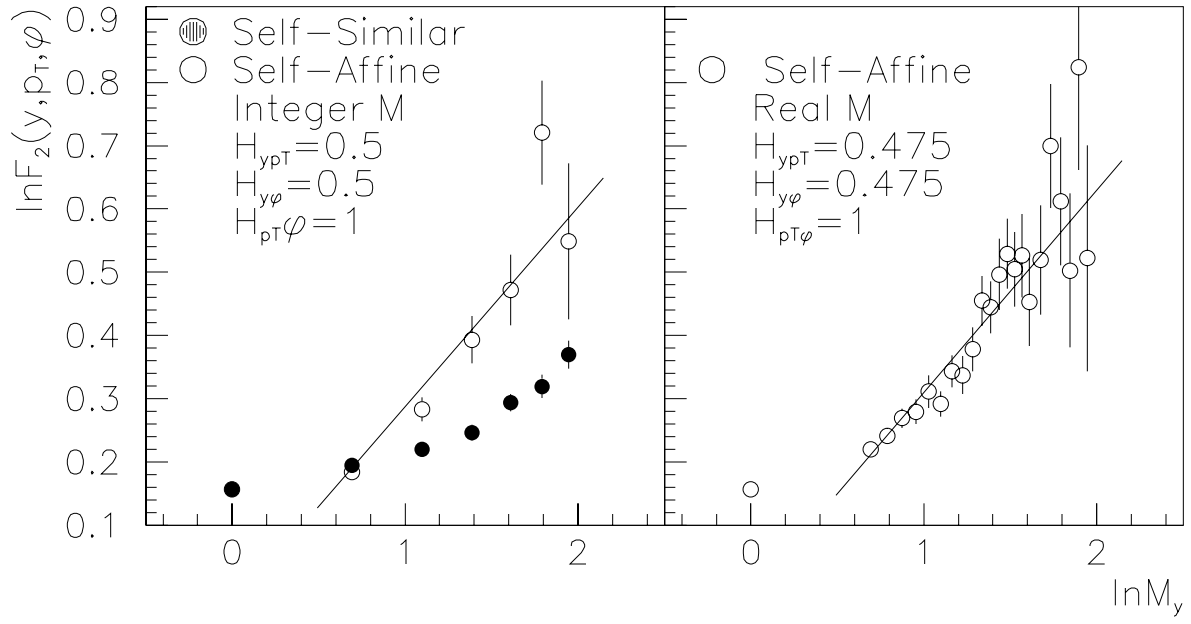
Fig.1

Fig. 2

Fig. 3

Fig.4